Biochemistry and Biophysics Reports 37 (2024) 101647

Contents lists available at ScienceDirect

Biochemistry and Biophysics Reports

journal homepage: www.elsevier.com/locate/bbrep

Identification of novel potential drugs for the treatment and prevention of osteoarthritis

Xiaosong Han [a,*], Fan Bai [a], Peng Li [a], Xiaojin Bai [a], Yanli Zhang [b], Wenmin Wang [b]

[a] Department of Osteology, the First People's Hospital of Zunyi, Zunyi, Guizhou, 563099, China
[b] Biological Medicine Research and Development Center, Yangtze Delta of Zhejiang, Hangzhou, Zhejiang, 314006, China

ARTICLE INFO

Keywords:
Osteoarthritis
Bioinformatics analysis
Differentially expressed genes
Tetrachlorodibenzodioxin
Valproic acid

ABSTRACT

Objectives: Osteoarthritis (OA) is characterized by a high prevalence, poor prognosis, and a propensity to lead to disability. Despite the availability of standard therapies, they are associated with potential side effects and don't provide a complete cure for patients. Consequently, there is an urgent demand for the development of novel drugs.

Method: The gene expression profiles (GSE64394, GSE178557 and GSE215039) of normal and OA chondrocytes samples were downloaded from the Gene Expression Omnibus (GEO) database. Differentially expressed genes (DEGs) were identified by the "LIMMA" R package. Gene Ontology (GO), Kyoto Encyclopedia of Genes and Genomes (KEGG) enrichment were conducted using the R package clusterProfiler. A protein-protein (PPI) interaction network was performed to identify hub genes by using the Search Tool for the Retrieval of Interacting Genes (STRING) and Cytoscape. Small molecule compounds linked to OA were predicted through the NetworkAnalyst platform. Finally, molecular docking was conducted using AutoDock and Pymol software.

Results: We identified 98 DEGs primarily implicated in endochondral ossification, extracellular matrix degradation, and Wnt signaling pathways. 23 DEGs were closely associated with OA, and 10 hub genes were found to be potential drug targets for OA. Two new targeted compounds, tetrachlorodibenzodioxin (TCDD) and valproic acid (VPA), were screened. And they both exhibited strong binding affinity to their respective targets.

Conclusions: Reducing exposure to TCDD could be a crucial strategy in preventing OA, and VPA has gained recognition as a novel drug candidate for OA treatment.

1. Introduction

Osteoarthritis (OA) is a prevalent chronic joint disease characterized by progressive joint pain, joint stiffness, and joint deformities, ultimately leading to physical disability and significantly impacting patients' quality of life [1]. It is estimated that nearly 250 million people worldwide currently suffer from OA, and this number continues to grow [2,3]. Moreover, one in four people with OA will eventually experience varying degrees of disability. The pathogenesis of OA is complex and primarily encompasses progressive cartilage degeneration, synovial inflammation, and structural changes in subchondral bone, including remodeling and sclerosis [4]. A mounting body of evidence suggests that chondrocyte, the sole cell type within articular cartilage, dysfunction can result in extracellular matrix (ECM) degradation and the secretion of inflammatory cytokines, ultimately culminating in cartilage degeneration [5]. In addition, the extent of chondrocyte apoptosis exhibits a direct correlation with the severity of OA [6]. While some methods for ameliorating OA symptoms exist, including drug therapy and joint replacement, their effectiveness is constrained, falling short of preventing the onset of OA and impeding its progression [7]. Moreover, the side effects and limitations of these therapies are difficult to solve [8]. Hence, it is crucial and pressing to investigate potential drug targets for the discovery and development of novel OA therapeutics.

In light of the rapid advancement of high-throughput sequencing technology, gene chip, and RNA-seq have become integral tools for investigating the molecular mechanisms underlying various diseases, screening for new biomarkers, and identifying potential drug targets [9,10]. However, due to sample size limitations and inter-sample variation, sequencing results for the same disease may not be entirely consistent. To this end, some researchers have integrated the results of several similar studies through bioinformatics methods for data re-mining to obtain new information [11]. To our knowledge, while a few articles

* Corresponding author.
E-mail address: Hanxiaosong2023@163.com (X. Han).

https://doi.org/10.1016/j.bbrep.2024.101647
Received 23 October 2023; Received in revised form 27 December 2023; Accepted 15 January 2024

have examined the relationship between OA and immune infiltration, there has been limited research aimed at screening drug targets for the prediction of innovative therapeutic agents for OA [12,13]. Therefore, the exploration of novel drug through bioinformatics approaches may be an effective strategy for the development of therapeutic interventions for OA.

In this study, a bioinformatics approach was utilized to develop a novel drug for the treatment of OA by integrating several datasets from the Gene Expression Omnibus (GEO) database. Screening and enrichment analysis of differentially expressed genes (DEGs) by R package to assess the molecular mechanisms of OA, screening of Hub genes as potential drug targets by protein-protein interaction (PPI) network, and identification of potential interacting drugs based on the networkanalyst platform to identify promising potential drug candidates in the treatment of OA. Lastly, molecular docking is employed to predict the binding affinities and interaction modes between potential drugs and target proteins.

2. Materials and methods

2.1. Data Collection

OA-related mRNA data from OA and normal chondrocytes were collected by integrating RNA-seq data and microarray expression datasets. The microarray expression datasets were retrieved from the GEO database (https://www.ncbi.nlm.nih. gov/geo/). Specifically, gene expression profiles GSE64394 and GSE178557 were chosen from the Agilent and Affymetrix platforms, respectively. Additionally, RNA-seq data were acquired from the GEO database, specifically gene expression profiles (GSE215039) obtained on the Illumina platform.

2.2. Identification of DEGs

Data preprocessing was carried out on the three datasets using the sva package in the R software. This process involved the removal of batch effects between groups, followed by data standardization. Differential analyses of the three datasets were used by the R package limma (version 4.3.0) to determine DEGs with the criteria of $|\log2(FC)| > 1$ and adjusted p-value <0.05 [14]. DEGs from all datasets were visualized using volcano plots, implemented with the ggrepel package. Venn diagrams were generated using DEGs from the three datasets to further identify co-expressed genes. Following the approach outlined by Wu and Xi [15], we selected co-expressed genes based on the intersection of at least two expression profile datasets to mitigate the limitations associated with relying solely on a single dataset. Subsequently, we integrated the results for further biological function analysis.

2.3. Functional enrichment analysis

Functional analysis of the aforementioned co-expressed genes involved Gene Ontology (GO) and Kyoto Encyclopedia of Genes and Genomes (KEGG) enrichment analyses, conducted using the R package clusterProfiler. Statistically significant gene enrichment was defined as having a p-value <0.05 [16]. Visualization of the KEGG enrichment results was accomplished through the creation of bubble plots using the R package ggplot2.

2.4. Identification of OA-related DEGs

Genes associated with OA were sourced from the Gencards (https://www.genecards.org/) and Online Mendelian Inheritance in Man (OMIM, https://omim.org/) databases using the keyword "Osteoarthritis". Genes retrieved from Gencard were filtered based on a relevance score greater than or equal to the median. These genes were subsequently integrated with the OMIM database, resulting in a total of 2839 genes significantly linked to OA. The aforementioned genes were then intersected with the co-expressed genes to identify the DEGs associated with OA.

2.5. PPI analysis and identification of key hub genes

The OA-related differentially expressed genes were uploaded to the STRING database (https://string-db.org/), with the species set to "Homo sapiens" and the interaction threshold set to ≥ 0.4. The remaining parameters were kept as default to obtain protein interaction data. After importing the PPI data into Cytoscape software (version 3.9.1), genes with significant interactions in candidate modules, representing the central gene subnetwork in the PPI map, were identified as hub genes [17]. We applied the degree, MNC, closeness, and MCC algorithms from the cytoHubba plug-in within Cytoscape to identify hub genes. The top 10 hub genes and their sub-networks were selected.

2.6. Prediction of compounds associated with OA and molecular docking

Small molecule compounds linked to OA were predicted based on hub genes using the NetworkAnalyst analytics platform (https://www.networkanalyst.ca/), with candidate compounds ranked in descending order of degree score [18]. Docking interactions between targets (key hub genes) and OA-related compounds were determined using AutoDock and visualized using Pymol software [19]. The most suitable conformation was selected based on the docking score and the rationality of molecular conformation.

2.7. Validation of drug-likeness and toxicity parameters of candidate compounds

Utilizing the ADMETlab 2.0 database (https://admetmesh.scbdd.com/) and the ProTox-II (https://tox-new.charite.de/protox_II/) databases, we performed drug-likeness and toxicity assessments on the identified candidate compounds. The pertinent parameters considered encompass the Lipinski Rule, Pfizer Rule, Human ether-a-go-go-related gene (hERG), Human Hepatotoxicity (H-HT), Drug-Induced Liver Injury (DILI), and Eye Corrosion.

3. Results

3.1. Differential expression analysis in OA

Because the dysfunction of chondrocytes is a primary characteristic of OA, we opted for three recently published or less-studied datasets pertaining to chondrocytes in OA from the GEO database. A total of 14 chondrocyte samples and 11 OA cell samples (GSE64394: 5 CK/2 OA; GSE178557: 4 CK/4 OA; GSE215039: 5 CK/5 OA) were obtained based on the mRNA microarray datasets (GSE64394 and GSE178557) and RNA-seq dataset (GSE215039) (Table 1). By comparing differential gene expression between diseased and normal tissues, potential biomarkers can be identified, shedding light on the underlying biological processes associated with disease initiation and progression. The results of DEGs identification in the three datasets are presented in Fig. 1. The GSE64394 dataset yielded 537 DEGs, comprising 271 up-regulated and 266 down-regulated genes (Fig. 1A). The same set of 537 DEGs was observed in GSE178557, with 266 up-regulated and 271 down-regulated

Table 1
GEO datasets of OA patients.

Accession ID	Dataset type	Platform	CK[a]	OA[b]
GSE64394	mRNA Microarray	Agilent	5	2
GSE215039	RNA-seq	Illumina	5	5
GSE178557	mRNA Microarray	Agilent	4	4

[a] CK (Normal chondrocytes).
[b] OA (Chondrocytes from OA patients).

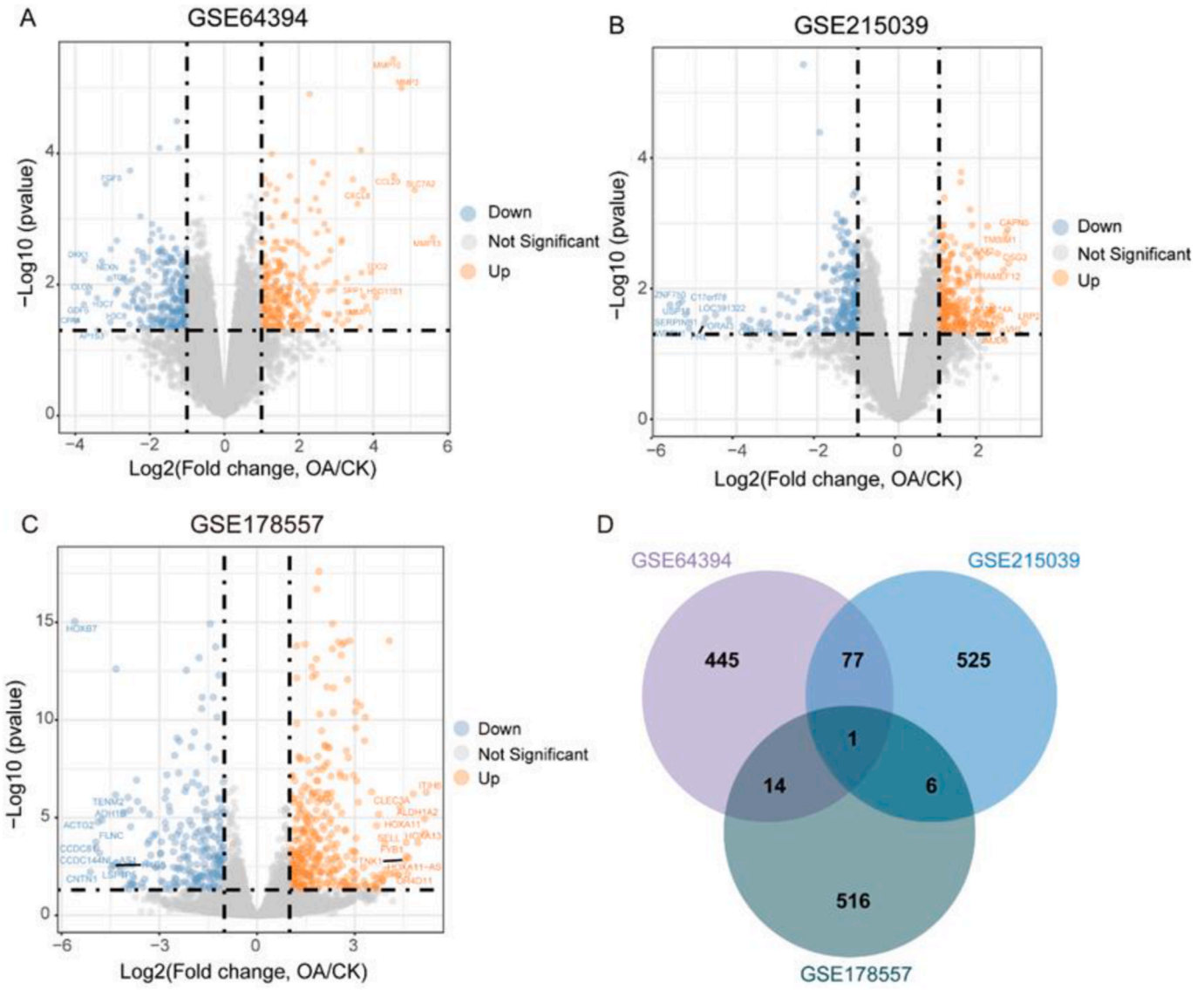

Fig. 1. Identification of common differentially expressed genes (DEGs) in three independent datasets. (A–C) Volcano plot for the DEGs in GSE64394 (A), GSE215039 (B), and GSE178557 (C) datasets when comparing osteoarthritis (OA) to normal chondrocyte. The orange and blue data points in the volcano plot represent upregulated and downregulated genes respectively screened based on $|Log2FC| > 1$ and the adjusted p-value <0.05. The grey data points represent genes with no significant difference. (D) Venn diagram of common DEGs in the 3 datasets; a total of 98 DEGs overlapped in at least 2 datasets.

genes (Fig. 1B). In GSE215039, we identified 609 DEGs, consisting of 377 up-regulated and 232 down-regulated genes (Fig. 1C). To enhance result reliability, we screened for DEGs commonly expressed in the three datasets, yielding only one significant gene, ALPL (Fig. 1D). This gene is upregulated in OA and has been proven to be a biomarker for OA. Therefore, we selected the intersection of at least two datasets to identify the final set of DEGs, resulting in a total of 98 co-expressed DEGs. Among these genes, the significantly upregulated genes include MMP13, MMP3, and ALDH1A2, while the downregulated genes include PRL, ACTG2, and FLNC.

3.2. Functional enrichment analysis of Co-expressed DEGs

We conducted GO and KEGG enrichment analysis on the 98 co-expressed DEGs to unveil the functions and biological processes associated with them. The GO bar graph displays the top 10 significantly enriched pathway terms in the biological process (BP), cellular component (CC), and molecular function (MF) categories (Fig. 2A). In the BP category, DEGs were primarily associated with processes such as endochondral ossification, replacement ossification, ECM organization, and extracellular structural organization. Within the CC category, DEGs showed strong associations with Z-discs, sarcomeres, collagen-containing ECM, I-bands, and myofibrils. In the MF category, DEGs were primarily linked to cyclic-nucleotide phosphodiesterase (PDE) activity, Wnt-protein binding and actin binding. KEGG enrichment analysis (Fig. 2B) revealed that DEGs were predominantly enriched in pathways such as glycine, serine and threonine metabolism, cytokine-cytokine receptor interactions, ferroptosis and the Wnt signaling pathway, which may be associated with the onset and progression of OA. These results indicate that OA is primarily associated with biological processes such as endochondral ossification, ECM degradation, and muscle tissue injury. The underlying mechanisms are potentially connected to the Wnt signaling pathway, ferroptosis, and cAMP or cGMP signaling pathways inhibited by PDE.

Fig. 2. The enrichment analysis of common DEGs. (A) Significantly enriched Gene Ontology (GO) pathways. Blue bars, Biological Process; red bars, Cellular Component; green bars, Molecular Function. (B) The results of KEGG enrichment for DEGs. P-value <0.05 was considered statistically significant.

3.3. Screening of OA-associated DEGs, PPI network analysis and selection of hub genes

In an effort to identify genes strongly linked to OA, a venny diagram analysis of 2839 OA-associated disease genes from the OMIM and Genecard databases and the previously identified 98 co-expressed DEGs was conducted. As shown in Fig. 3A, we screened 23 DEGs related to OA. The PPI network of the 23 DEGs was constructed using the STRING database (Fig. 3B), and the top 10 candidate hub genes were identified through calculations of degree, MNC, closeness, and MCC using the cytoHubba plugin. These hub genes include BMP2, MMP13, COL2A1, ALPL, MMP3, DLX5, SOX5, PRL, CP, and SERPINA1 (Table 2). Fig. 3C illustrates the PPI network among the 10 hub genes, categorized into two groups. CP and SERPINA1 constitute one group, while the remaining hub genes comprise the other.

3.4. Identification of potential OA candidate compounds

Compounds that may interact with the 10 hub genes were screened as candidate compounds for OA through the NetworkAnalyst platform. The target interactions of these candidate compounds are detailed in Table 3. The top four compounds, ranked based on the degree score, were dexamethasone (Dex), estradiol, tetrachlorodibenzodioxin (TCDD), and valproic acid (VPA) (Fig. 4). It's worth noting that Dex and estradiol have been utilized in clinical practice or clinical trials for OA treatment [20,21]. Thus, our primary focus of investigation centered on TCDD and VPA. In addition, it has been proposed that the focus of OA treatment should extend beyond cartilage alone, recognizing the pivotal role played by synovium in the initiation and progression of OA [22]. Consequently, we delved deeper into the impact of VPA and TCDD on common targets within both cartilage and synovial tissues. Utilizing information extracted from the aforementioned literature, we identified 35 genes exhibiting similar OA-responsive expression patterns in both tissues. Subsequently, the interactions of VPA and TCDD with these genes were scrutinized using the NetworkAnalyst platform. The results revealed that TCDD exhibited interactions with 13 genes, while VPA interacted with 11 genes (Table 4). This observation implies that the effects of VPA and TCDD on synovium are concordant with those on cartilage.

Table 2
Scores for the top 10 hub genes in different calculations.

Gene name	MCC	MNC	Degree	Closeness
BMP2	15	5	6	6.5
MMP13	14	5	5	6
COL2A1	14	5	5	6
ALPL	8	4	4	5.5
MMP3	6	3	3	5
DLX5	3	2	3	5
SOX5	3	2	3	4.8
PRL	1	1	1	3.8
CP	3	1	3	3
SERPINA1	1	1	1	2

MCC: Maximum Clique Centrality, MNC: Maximum Neighborhood Component.

3.5. Interaction of candidate compounds with hub genes

To assess whether TCDD and VPA engage in direct interactions with their respective hub genes, we conducted molecular docking experiments between them. Notably, TCDD exhibits a stronger binding affinity to its hub genes when compared to VPA. The binding affinity scores of

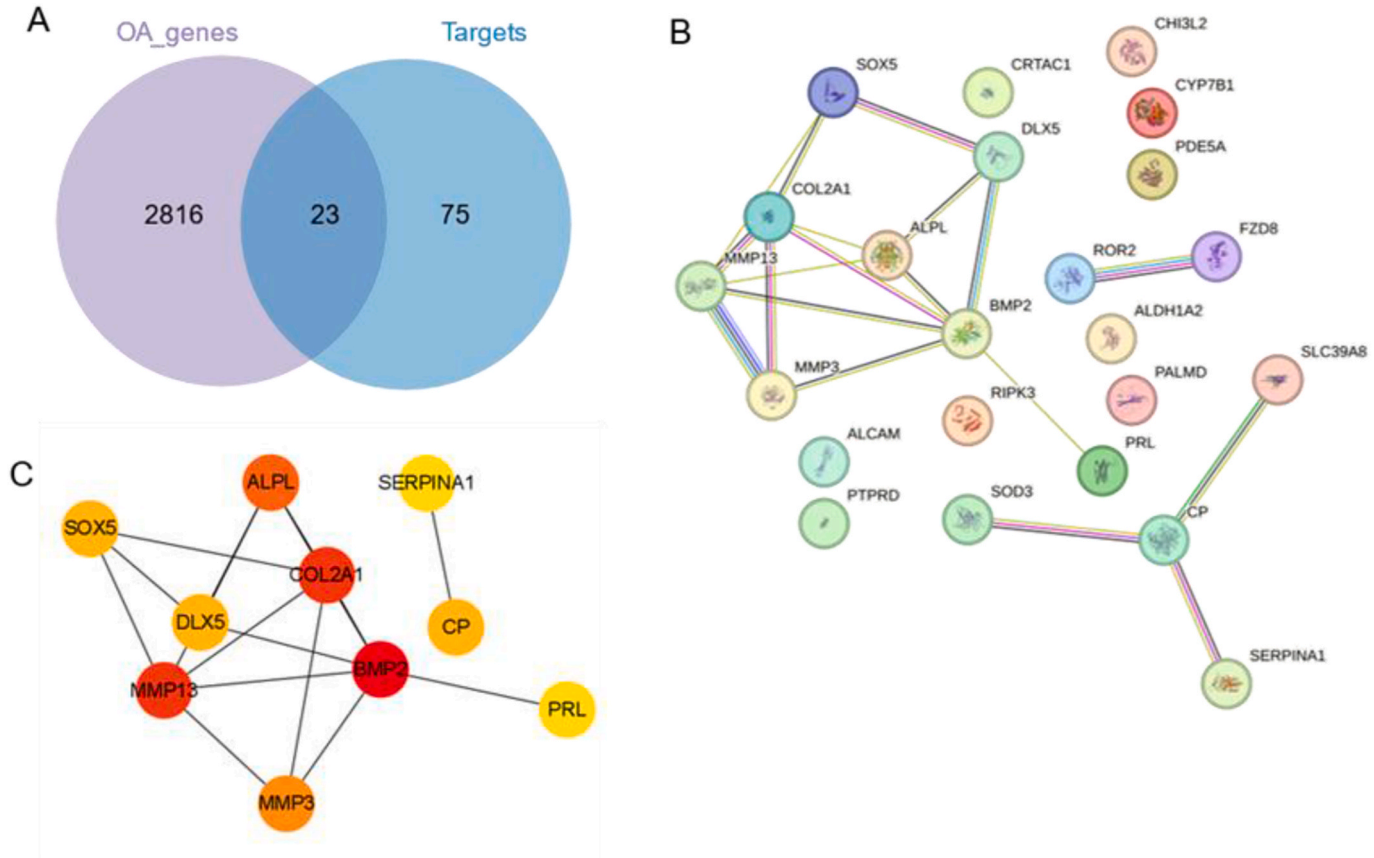

Fig. 3. The protein–protein interaction (PPI) network of OA-associated DEGs and hub genes. (A) Intersection of 98 DEGs and 2839 OA-related genes. (B) PPI network of 23 OA-associated DEGs. (C) Top 10 OA-related hub genes. The network was analyzed by the cytoHubba plugin of Cytoscape software with the method of degree, MNC, closeness and MCC. The color gradient from red to yellow signifies a transition from high to low degree values.

Table 3
Candidate compounds and their targets.

Compound ID	Compound	Degree	Target
D003907	Dexamethasone	8	ALPL, BMP2, COL2A1, DLX5, MMP13, MMP3, PRL, SERPINA1
D004958	Estradiol	7	ALPL, BMP2, CP, MMP13, MMP3, PRL, SERPINA1
D013749	Tetrachlorodibenzodioxin	7	ALPL, BMP2, COL2A1, CP, MMP13, MMP3, SERPINA1
D014635	Valproic Acid	7	ALPL, BMP2, COL2A1, DLX5, MMP13, SERPINA1, SOX5
D002104	Cadmium	6	ALPL, BMP2, CP, MMP13, PRL, SERPINA1
D002117	Calcitriol	6	ALPL, BMP2, CP, MMP13, MMP3, SERPINA1
D014212	Tretinoin	6	ALPL, BMP2, COL2A1, CP, MMP3, SOX5
D003300	Copper	5	CP, MMP13, MMP3, PRL, SERPINA1
D011374	Progesterone	5	ALPL, BMP2, CP, MMP3, PRL
C006780	Bisphenol A	5	ALPL, CP, MMP3, PRL, SOX5
D016604	Aflatoxin B1	5	ALPL, BMP2, CP, MMP3, SOX5
D011794	Quercetin	5	BMP2, COL2A1, CP, MMP13, MMP3
D018501	Antirheumatic Agents	5	COL2A1, CP, DLX5, MMP3, SERPINA1
C059514	Resveratrol	5	BMP2, COL2A1, MMP13, MMP3, SERPINA1
D016572	Cyclosporine	5	ALPL, COL2A1, CP, MMP3, SOX5
D001564	Benzo(*a*)pyrene	5	COL2A1, CP, MMP13, MMP3, SOX5
C459179	4-(5-benzo(1,3)dioxol-5-yl-4-pyridin-2-yl-1H-imidazole-2-yl) benzamide	5	ALPL, BMP2, COL2A1, DLX5, SOX5

TCDD ranged from −8 to −4 kcal/mol, with the highest binding affinity observed for MMP3 at −7.74 kcal/mol (Table 5). In contrast, the binding affinity scores between VPA and its seven target genes ranged from 2 to 3, with the strongest binding observed for MMP13 and SERPINA1 at −2.93 and −3.01 kcal/mol. TCDD interacts with residues CYS-80, LEU-722, GLY-2237, CYS-64, SER-266, GLU-199, and THR-707 through hydrogen bonding of the side chains, respectively, facilitating binding to BMP2, MMP3, MMP13, COL2A1, ALPL, SERPINA1, and CP (Fig. 5). VPA interacts with residues ARG-16, ARG-558, LYS-2143, CYS-85, GLN-442 and LYS-368 through hydrogen bonding of the side chains, respectively, enabling binding to BMP2, SOX5, MMP13, COL2A1, ALPL and SERPINA1 (Fig. 6). In addition, VPA interacts with DLX5 through two conventional hydrogen bonding with two residues GLN-153 and LYS-191. In summary, our findings indicate that TCDD promotes while VPA inhibits the progression of OA by directly binding to the hub genes.

3.6. The verification of drug-likeness and toxicity on candidate compounds

The drug-likeness analysis results indicate that VPA meets the Lipinski Rule, the Pfizer Rule, and the GSK Rule. In contrast, TCDD only satisfies the Lipinski Rule, suggesting that VPA holds promise as a potential therapeutic drug (Table 6). Furthermore, VPA exhibits lower toxicity and places a reduced burden on the liver, though it should be noted for its potential eye irritancy and corrosion. Conversely, TCDD is highly toxic, carcinogenic, and poses a significant risk of liver injury. These findings serve to corroborate our earlier conjectures.

4. Discussion

OA is of exceptional concern due to its exceedingly high prevalence, often ranking among the top three health threats alongside cardiovascular disease and cancer [23]. Consequently, OA treatment presents a formidable challenge. Clinical symptoms allow the categorization of OA into two primary structural phenotypes: inflammation and cartilage-related damage [24]. Current treatments are primarily aimed at alleviating these symptoms and managing pain but do not offer a definitive cure [25]. Significant advancements in high-throughput sequencing technology and microarray technology have substantially enhanced our comprehension of OA's pathogenesis, offering promise for early diagnosis and targeted treatment. In the current study, we employed bioinformatics analysis to pinpoint hub genes associated with OA and conducted a screening for potential drug candidates and pathogenic compounds.

Through amalgamating data from three OA datasets sourced from the GEO database, we identified 98 co-expressed DEGs and assessed their functions by GO and KEGG enrichment analyses. GO analysis revealed that DEGs are predominantly associated to endochondral ossification and ECM degradation, recognized as pivotal contributors to OA pathogenesis [26]. The mechanism may involve chondrocyte apoptosis [27], KEGG results also showed that DEGs were significantly enriched in ferroptosis pathway. In addition, our findings indicate a significant correlation between PDE activity and OA. PDE inhibitors exhibited a favorable anti-inflammatory effect, preventing cAMP degradation [28], suppressing TNF-β-induced inflammatory activation and degradation of collagen in chondrocytes [29]. Remarkably, DEGs displayed substantial associations with muscle tissue structures, including myogenic fibers, Z-discs, and muscle ganglia. These findings indicate a potential influence of skeletal muscle on OA progression, aligning with the observations made by Liu et al. [30]. Furthermore, both KEGG and GO enrichment analyses unveiled significant enrichment of DEGs in the Wnt signaling pathway, indicating its substantial involvement in OA development. Prior research has documented that both excessive and insufficient activation of the Wnt signaling pathway can lead to chondrocyte apoptosis and contribute to OA. On one hand, Wnt16 inhibits OA progression via the PCP/JNK-mTORC1-PTHrP cascade, while on the other, it counteracts excessive typical Wnt activation, thus protecting OA cartilage [31,32]. In summary, the Wnt signaling pathway may trigger chondrocyte apoptosis, leading to cartilage damage and ECM degradation, ultimately culminating in OA.

We screened four highly top-rated compounds by evaluating their interaction with hub genes through the NetworkAnalyst platform. Among them, Dex stands out as a glucocorticoid anti-inflammatory drug with clinical applications in knee OA treatment. It offers short-term pain relief and functional improvement, but prolonged use may entail specific side effects and potentially exacerbate OA symptoms [33]. Estradiol, an estrogen variant, exhibits associations with structural changes linked to knee OA in women. Additionally, research has demonstrated that estradiol curbs apoptosis in articular chondrocytes of female mice, consequently hindering OA cartilage degeneration [34]. However, there was no significant correlation between estradiol and OA risk in men [35]. TCDD, a highly toxic and broadly distributed environmental pollutant, has been implicated by Yang et al. in mediating apoptosis in rabbit chondrocytes via ROS and NO-dependent pathways [36]. Apoptosis of chondrocytes represents a pivotal pathogenetic mechanism in OA, aligning with our study's findings. Furthermore, our investigation reveals that TCDD exhibits a pronounced affinity for binding to MMP3,

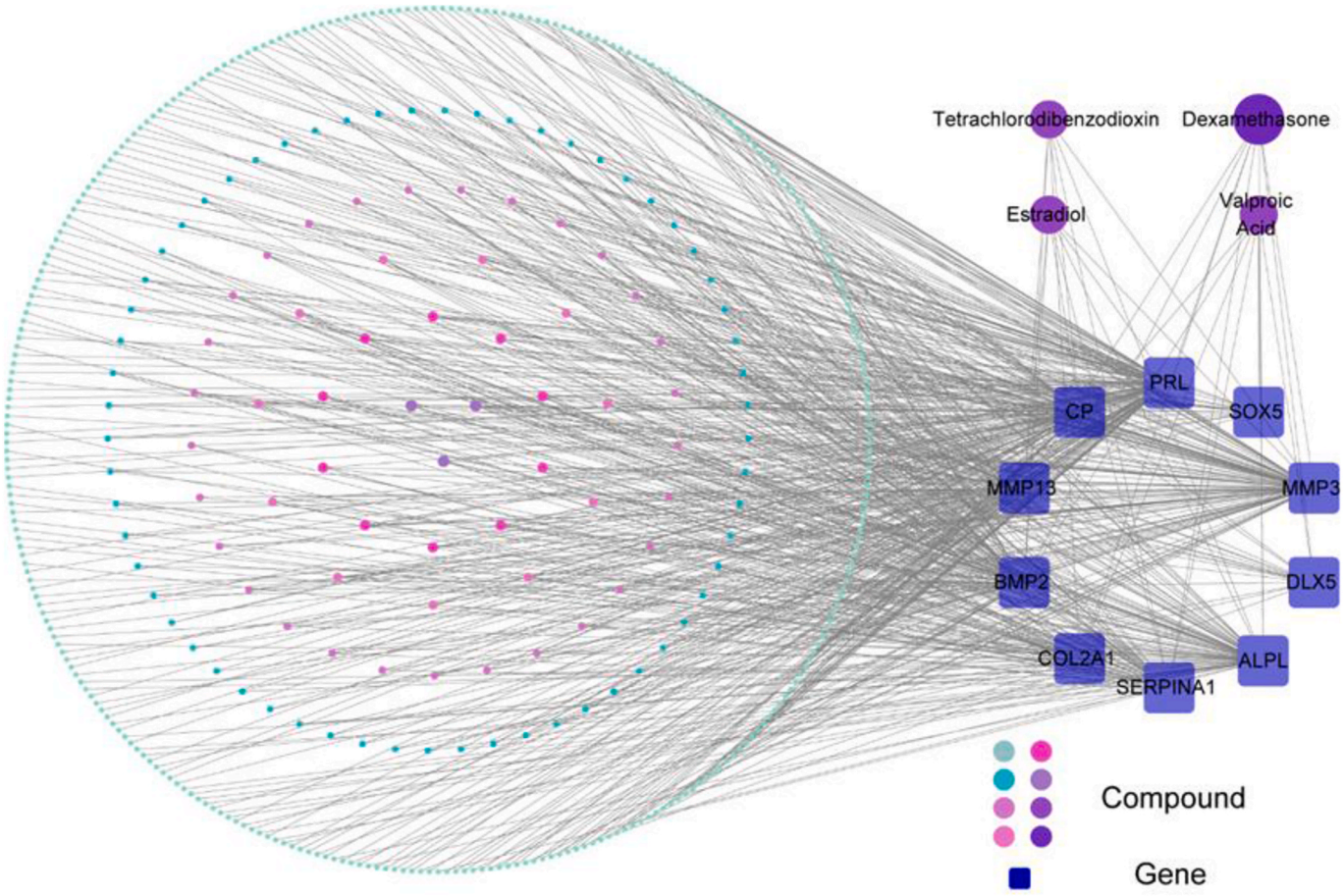

Fig. 4. Interaction networks between compounds and hub genes. Genes are represented as rectangles, while compounds are represented as circles. The size and color of each circle correspond to the respective degree value.

Table 4
Interaction of TCDD and VPA with genes exhibiting comparable expression patterns in response to OA.

Compound ID	Compound	Degree	Target
D013749	TCDD	13	APOD, ASPM, C1QB, CDK1, CKAP2L, GPT2, KLF15, LRRC15, MMP3, MSR1, PBK, TNFAIP6, TOP2A
D014635	VPA	11	ANLN, ASPM, C1QB, GJB2, KLF15, LRRC15, MMP3, PBK, PFKFB3, ST6GALNAC5, TOP2A

MMP13, and BMP2. MMP3 and MMP13 are closely associated with ECM degradation, while BMP2 plays a role in cartilage formation and apoptosis [37]. Consequently, TCDD may foster OA development by triggering ECM degradation and suppressing cartilage formation.

VPA, an inhibitor of histone deacetylase (HDAC), serves as a preventive measure against cartilage degradation by inhibiting cytokine-induced metalloproteinase expression in human articular chondrocytes and bovine nasal cartilage explants [38,39]. Earlier research also proposes SCRG1 as a novel drug target for OA synovitis and identifies VPA as a potential targeted therapeutic agent for SCRG1 [40]. Furthermore, VPA exerts anti-OA effects by modulating the miR-302d-3p/ITGB4 axis and stimulating the PI3K-AKT pathway [41]. An intriguing observation is that both Dex and VPA are employed in the treatment of epilepsy and migraines, suggesting that in certain contexts, they may exert similar effects [42,43]. These investigations present VPA as a promising avenue for developing effective treatments for OA. In our study, VPA targeted 7 hub genes, ranking second only to Dex. Notably, VPA exhibited a stronger binding affinity for SERPINA1 and MMP13. Neutrophil elastase (NE) has been identified as a contributor to OA and represents a novel activator of MMP13, demonstrating greater potency compared to the classical collagenase activator MMP3 [44]. Alpha-1-antitrypsin (AAT), the protein encoded by the *SERPINA1* gene, serves as a potent inhibitor of NE with significant chondrogenic and protective properties, and the absence of AAT in cartilage has a detrimental impact on OA progression [45]. AAT fosters the transcription of COL2A1, ACAN and SOX9, while concurrently down-regulating MMP13 gene expression through the activation of cAMP/PKA/CREB signaling pathway and the inhibition of the Wnt/β-catenin pathway to exert chondroprotective effects in OA [46]. Interestingly, our study observed a decrease in PDE activity, resulting in reduced cAMP degradation. Therefore, we hypothesized that VPA primarily averts cartilage degradation by specifically targeting SERPINA1. This action involves the activation of cAMP/PKA/CREB signaling pathway and the inhibition of the Wnt/β-collagen signaling pathway, which results in up-regulation of cartilage differentiation genes and down-regulation of matrix metalloproteinase genes. Notably, research has demonstrated that VPA modulates the production of fatty acids by gut microbes, thereby affecting individuals with epilepsy undergoing VPA treatment [47]. The restructuring of the gut microbiota and its associated metabolites significantly influences the initiation and advancement of OA [48,49]. Therefore, gut microbiota may play a role in the therapeutic effects of VPA on OA.

In this study, we curated DEGs from three distinct datasets sourced from the GEO database. Subsequently, we conducted a comprehensive screening process to identify potential therapeutic applications of VPA for OA and to investigate the pathogenic properties of TCDD. Moreover, molecular docking was carried out to delve into the interactions

Table 5
Molecular docking parameters of candidate compounds with hub genes.

Ligand	Receptor	PDB ID	Binging Affinity (kcal/mol)	Bonding Length(Å)	Amino Acid Residue	Interaction
TCDD	BMP2	4N1D	−5.42	2.2	CYS-80	Hydrogen bond
TCDD	MMP3	1G49	−7.74	2.7	LEU-722	Hydrogen bond
TCDD	MMP13	3O2X	−5.84	3	GLY-2237	Hydrogen bond
TCDD	COL2A1	5NIR	−4.8	2.7	CYS-64	Hydrogen bond
TCDD	ALPL	7YIX	−4.57	2	SER-266	Hydrogen bond
TCDD	SERPINA1	5NBU	−4.51	2.9	GLU-199	Hydrogen bond
TCDD	CP	2J5W	−4.14	3.3	THR-707	Hydrogen bond
VPA	BMP2	4N1D	−1.94	2	ARG16	Hydrogen bond
VPA	SOX5	Model[1]	−2.67	2.2	ARG558	Hydrogen bond
VPA	MMP13	3O2X	−2.93	1.8	LYS2143	Hydrogen bond
VPA	COL2A1	5NIR	−1.96	2	CYS85	Hydrogen bond
VPA	ALPL	7YIX	−1.88	1.6	GLN442	Hydrogen bond
VPA	SERPINA1	5NBU	−3.01	1.9	LYS368	Hydrogen bond
VPA	DLX5	4RDU	−2.12	1.8	GLN153	Hydrogen bond
				2.1	LYS191	Hydrogen bond

TCDD: tetrachlorodibenzodioxin, VPA: valproic acid. [1]Model indicates that the structure of the protein is unknown and we constructed a structural model based on its sequence.

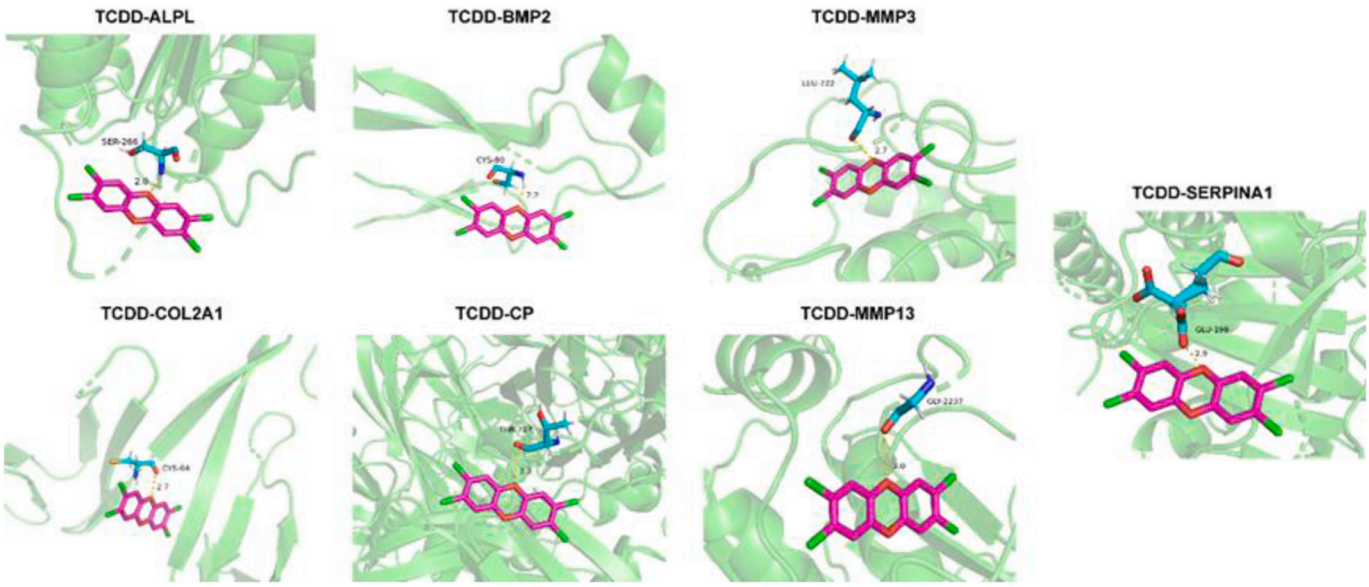

Fig. 5. Molecular docking simulation for tetrachlorodibenzodioxin (TCDD) and hub genes. The abbreviations represent the amino acid residues crucial for ligand-receptor binding, while the numbers indicate the respective binding lengths.

between compounds and their respective targets, and possible pathogenic mechanisms of TCDD and potential therapeutic mechanisms of VPA were predicted in conjunction with previous studies. Our study has offered novel strategies for the prevention and treatment of OA. Nonetheless, it is essential to acknowledge the limitations of this study. The datasets were obtained from various platforms, introducing variations in data quality that could potentially affect the robustness of the results. Secondly, to substantiate our findings, additional in vitro and in vivo experiments are warranted for result validation.

5. Conclusions

In conclusion, we identified a total of 98 common DEGs from three existing datasets through bioinformatics. They primarily participate in processes related to endochondral ossification, ECM degradation, chondrocyte apoptosis induced by ferroptosis, and the Wnt and cAMP signaling pathways. Among these DEGs, we identified ten promising hub genes for OA, including upregulated genes such as BMP2, MMP13, ALPL, MMP3, DLX5, SOX5, CP, and SERPINA1, as well as downregulated genes like COL2A1 and PRL. A novel OA-targeted therapeutic drug (VPA) and a potential pathogenic small molecule compound (TCDD) were identified through compound-target interactions, and preliminary validation was carried out by molecular docking. These results hold promise for advancing strategies aimed at OA prevention and the creation of innovative therapeutic drugs for OA treatment.

Ethics standards

Not applicable.

Consent for publication

Not applicable.

Availability of data and materials

The raw data of the three datasets (accession numbers GSE64394, GSE178557 and GSE215039) were downloaded from the GEO repository (https://www.ncbi.nlm.nih.gov/geo/). All data are publicly accessible.

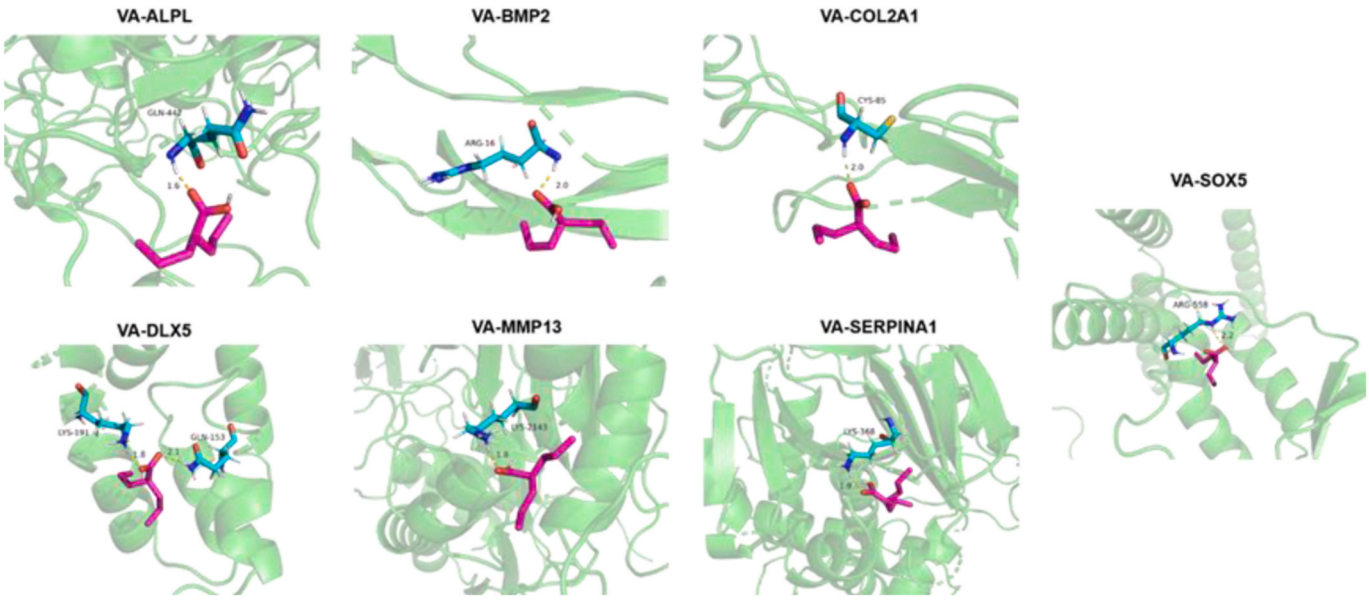

Fig. 6. Molecular docking simulation for valproic acid (VPA) and hub genes. The abbreviations represent the amino acid residues crucial for ligand-receptor binding, while the numbers indicate the respective binding lengths.

Table 6
The verification of drug-likeness and toxicity on candidate compounds.

Parameters	TCDD	VPA
Lipinski Rule	Accepted	Accepted
Pfizer Rule	Rejected	Accepted
GSK Rule	Rejected	Accepted
Predicted Toxicity Class	1	4
Carcinogenicity	Active	Inactive
hERG Blockers	Inactive	Inactive
H-HT	Negative	Negative
DILI	High risk	Low risk
Eye Irritation	Irritants	Irritants
Eye Corrosion	Noncorrosives	Corrosives

H-HT: Human Hepatotoxicity, DILI: Drug Induced Liver Injury.

Formatting of funding sources

This research did not receive any specific grant from funding agencies in the public, commercial, or not-for-profit sectors.

CRediT authorship contribution statement

Xiaosong Han: Conceptualization, Writing – original draft. **Fan Bai:** Conceptualization, Writing – original draft. **Peng Li:** Data curation, Formal analysis, Software. **Xiaojin Bai:** Data curation, Formal analysis, Software. **Yanli Zhang:** Data curation, Formal analysis, Software. **Wenmin Wang:** Supervision, Writing – review & editing.

Declaration of competing interest

The authors declare that they have no known competing financial interests or personal relationships that could have appeared to influence the work reported in this paper.

Data availability

Data will be made available on request.

Acknowledgements

Not applicable.

References

[1] W. Liu, A. Liu, X. Li, et al., Dual-engineered cartilage-targeting extracellular vesicles derived from mesenchymal stem cells enhance osteoarthritis treatment via miR-223/NLRP3/pyroptosis axis: toward a precision therapy, Bioact. Mater. 30 (2023) 169–183.
[2] D.J. Hunter, S. Bierma-Zeinstra, Osteoarthritis. Lancet 393 (10182) (2019) 1745–1759.
[3] A. Turkiewicz, I.F. Petersson, J. Bjork, et al., Current and future impact of osteoarthritis on health care: a population-based study with projections to year 2032, Osteoarthritis Cartilage 22 (11) (2014) 1826–1832.
[4] J. Clarke, Bone stresses out cartilage in OA, Nat. Rev. Rheumatol. 17 (5) (2021) 250.
[5] Z. Liu, J. Huang, X. Wang, et al., Dapagliflozin suppress endoplasmic reticulum stress mediated apoptosis of chondrocytes by activating Sirt1, Chem. Biol. Interact. 384 (2023) 110724.
[6] L. Tong, H. Yu, X. Huang, et al., Current understanding of osteoarthritis pathogenesis and relevant new approaches, Bone Res 10 (1) (2022) 60.
[7] A.J. Gibbs, B. Gray, J.A. Wallis, et al., Recommendations for the management of hip and knee osteoarthritis: a systematic review of clinical practice guidelines, Osteoarthritis Cartilage 31 (10) (2023) 1280–1292.
[8] N.E. Foster, L. Eriksson, L. Deveza, et al., Osteoarthritis year in review 2022: Epidemiology & therapy, Osteoarthritis Cartilage 31 (7) (2023) 876–883.
[9] A. Claveria-Cabello, J.M. Herranz, M.U. Latasa, et al., Identification and experimental validation of druggable epigenetic targets in hepatoblastoma, J. Hepatol. 79 (4) (2023) 989–1005.
[10] R. Wang, W. Liu, X. Liu, et al., Comparative analysis of whole genomes and transcriptomes of Microsporum canis from invasive dermatophytosis and tinea capitis, Emerg Microbes Infect 12 (1) (2023) 2219346.
[11] Y. Xiao, B. Zhang, J.M. Cloyd, et al., Novel drug candidate prediction for Intrahepatic Cholangiocarcinoma via hub gene network analysis and Connectivity Mapping, Cancers 14 (13) (2022).
[12] J. Wang, Q. Fan, T. Yu, et al., Identifying the hub genes and immune cell infiltration in synovial tissue between osteoarthritic and Rheumatoid Arthritic patients by bioinformatic approach, Curr Pharm Des 28 (6) (2022) 497–509.
[13] P. Cheng, S. Gong, C. Guo, et al., Exploration of effective biomarkers and infiltrating Immune cells in Osteoarthritis based on bioinformatics analysis, Artif. Cells, Nanomed. Biotechnol. 51 (1) (2023) 242–254.
[14] R. Gentleman, V.J. Carey, W. Huber, et al., Bioinformatics and Computational Biology Solutions Using R and Bioconductor, vol. 1, Springer, 2005.
[15] B. Wu, S. Xi, Bioinformatics analysis of differentially expressed genes and pathways in the development of cervical cancer, BMC Cancer 21 (1) (2021) 733.
[16] T. Wu, E. Hu, S. Xu, et al., clusterProfiler 4.0: a universal enrichment tool for interpreting omics data, Innovation 2 (3) (2021) 100141.
[17] P. Shannon, A. Markiel, O. Ozier, et al., Cytoscape: a software environment for integrated models of biomolecular interaction networks, Genome Res. 13 (11) (2003) 2498–2504.
[18] G. Zhou, O. Soufan, J. Ewald, et al., NetworkAnalyst 3.0: a visual analytics platform for comprehensive gene expression profiling and meta-analysis, Nucleic Acids Res. 47 (W1) (2019) W234–W241.
[19] G.M. Morris, R. Huey, W. Lindstrom, et al., AutoDock4 and AutoDockTools4: Automated docking with selective receptor flexibility, J. Comput. Chem. 30 (16) (2009) 2785–2791.

[20] S. Liu, C. Zhang, Y. Zhou, et al., MRI-visible mesoporous polydopamine nanoparticles with enhanced antioxidant capacity for osteoarthritis therapy, Biomaterials 295 (2023) 122030.
[21] K.E. Ackerman, V. Singhal, M. Slattery, et al., Effects of estrogen replacement on bone Geometry and Microarchitecture in Adolescent and Young Adult Oligoamenorrheic Athletes: a Randomized trial, J. Bone Miner. Res. 35 (2) (2020) 248–260.
[22] C. Li, Z. Zheng, Identification of novel targets of knee osteoarthritis Shared by cartilage and synovial tissue, Int. J. Mol. Sci. 21 (17) (2020).
[23] L.F. Callahan, K.R. Ambrose, A.L. Albright, et al., Public health interventions for osteoarthritis - updates on the osteoarthritis action Alliance's efforts to address the 2010 OA public health Agenda Recommendations, Clin. Exp. Rheumatol. 37 (Suppl 120) (2019) 31–39 (5).
[24] F.W. Roemer, M. Jarraya, J.E. Collins, et al., Structural phenotypes of knee osteoarthritis: potential clinical and research relevance, Skeletal Radiol. 52 (11) (2023) 2021–2030.
[25] M.A. Karsdal, J. Tambiah, D. Felson, et al., Reflections from the OARSI 2022 clinical trials symposium: the pain of OA-Deconstruction of pain and patient-reported outcome measures for the benefit of patients and clinical trial design, Osteoarthritis Cartilage 31 (10) (2023) 1293–1302.
[26] D. Yu, J. Hu, Z. Sheng, et al., Dual roles of misshapen/NIK-related kinase (MINK1) in osteoarthritis subtypes through the activation of TGFbeta signaling, Osteoarthritis Cartilage 28 (1) (2020) 112–121.
[27] R. Zhu, Y. Wang, Z. Ouyang, et al., Targeting regulated chondrocyte death in osteoarthritis therapy, Biochem. Pharmacol. 215 (2023) 115707.
[28] Z. Jenei-Lanzl, J. Zwingenberg, T. Lowin, et al., Proinflammatory receptor switch from Galphas to Galphai signaling by beta-arrestin-mediated PDE4 recruitment in mixed RA synovial cells, Brain Behav. Immun. 50 (2015) 266–274.
[29] J. Zhao, L. Duan, R. Wang, et al., Roflumilast prevents lymphotoxin alpha (TNF-beta)-induced inflammation activation and degradation of type 2 collagen in chondrocytes, Inflamm. Res. 69 (12) (2020) 1191–1199.
[30] J. Liu, Q.X. Lin, L.M. Lu, et al., [Effect of acupotomy intervention on the morphology and ultrastructure of rectus femoris muscle in rabbits with knee osteoarthritis], Zhong Guo Gu Shang 35 (3) (2022) 281–286.
[31] W. Tong, Y. Zeng, D.H.K. Chow, et al., Wnt16 attenuates osteoarthritis progression through a PCP/JNK-mTORC1-PTHrP cascade, Ann. Rheum. Dis. 78 (4) (2019) 551–561.
[32] G. Nalesso, B.L. Thomas, J.C. Sherwood, et al., WNT16 antagonises excessive canonical WNT activation and protects cartilage in osteoarthritis, Ann. Rheum. Dis. 76 (1) (2017) 218–226.
[33] Y. Peng, H. Jiang, H.D. Zuo, Factors affecting osteogenesis and chondrogenic differentiation of mesenchymal stem cells in osteoarthritis, World J Stem Cells 15 (6) (2023) 548–560.
[34] R. Dreier, T. Ising, M. Ramroth, et al., Estradiol inhibits ER stress-induced apoptosis in chondrocytes and contributes to a reduced osteoarthritic cartilage degeneration in female mice, Front. Cell Dev. Biol. 10 (2022) 913118.
[35] S.M. Hussain, F.M. Cicuttini, G.G. Giles, et al., Relationship between circulating sex steroid hormone concentrations and incidence of total knee and hip arthroplasty due to osteoarthritis in men, Osteoarthritis Cartilage 24 (8) (2016) 1408–1412.
[36] J.H. Yang, H.G. Lee, 2,3,7,8-Tetrachlorodibenzo-p-dioxin induces apoptosis of articular chondrocytes in culture, Chemosphere 79 (3) (2010) 278–284.
[37] S.Y. Chien, C.H. Tsai, S.C. Liu, et al., Noggin inhibits IL-1beta and BMP-2 expression, and attenuates cartilage degeneration and subchondral bone Destruction in experimental osteoarthritis, Cells 9 (4) (2020).
[38] A. Elseoudi, T. Nishida, T. Mizukawa, et al., Bipartite regulation of cellular communication network factor 2 and fibroblast growth factor 1 genes by fibroblast growth factor 1 through histone deacetylase 1 and fork head box protein A1, J Cell Commun Signal 15 (1) (2021) 81–91.
[39] K.L. Culley, W. Hui, M.J. Barter, et al., Class I histone deacetylase inhibition modulates metalloproteinase expression and blocks cytokine-induced cartilage degradation, Arthritis Rheum. 65 (7) (2013) 1822–1830.
[40] G. Liu, G. He, J. Zhang, et al., Identification of SCRG1 as a potential therapeutic target for human synovial inflammation, Front. Immunol. 13 (2022) 893301.
[41] L. Sun, W. Zheng, Q.D. Liu, et al., Valproic acid protects chondrocytes from LPS-Stimulated damage via regulating miR-302d-3p/ITGB4 Axis and mediating the PI3K-AKT signaling pathway, Front. Mol. Biosci. 8 (2021) 633315.
[42] F. Wang, H. Zhang, L. Wang, et al., Intravenous sodium valproate for acute migraine in the emergency department: a meta-analysis, Acta Neurol. Scand. 142 (6) (2020) 521–530.
[43] D. Goel, A. Srivastava, A. Aledo-Serrano, et al., Pharmacotherapy for SARS-CoV-2 and Seizures for drug Repurposing Presumed on Mechanistic targets, Curr. Mol. Pharmacol. 15 (6) (2022) 832–845.
[44] M.K. Kaneva, Neutrophil elastase and its inhibitors-overlooked players in osteoarthritis, FEBS J. 289 (1) (2022) 113–116.
[45] D.J. Wilkinson, A.M.D. Falconer, H.L. Wright, et al., Matrix metalloproteinase-13 is fully activated by neutrophil elastase and inactivates its serpin inhibitor, alpha-1 antitrypsin: Implications for osteoarthritis, FEBS J. 289 (1) (2022) 121–139.
[46] M.K. Kaneva, M.M. Muley, E. Krustev, et al., Alpha-1-antitrypsin reduces inflammation and exerts chondroprotection in arthritis, FASEB J 35 (5) (2021) e21472.
[47] P. Poolchanuan, P. Unagul, S. Thongnest, et al., An anticonvulsive drug, valproic acid (valproate), has effects on the biosynthesis of fatty acids and polyketides in microorganisms, Sci. Rep. 10 (1) (2020) 9300.
[48] M. Liu, G. Matuszek, M. Azcarate-Peril, et al., An exploratory Case-Control study on the associations of Bacterially-derived Vitamin K Forms with the Intestinal Microbiome and Obesity-related osteoarthritis, Curr. Dev. Nutr. 7 (3) (2023) 100049.
[49] M. Jeyaraman, P. Ram, N. Jeyaraman, et al., The gut-joint Axis in osteoarthritis, Cureus 15 (11) (2023) e48951.